# Implementation, Evaluation, and Applications of Linearization-based Self-Interference Cancellation for Full Duplex Radios

*A Project Report*

*submitted by*

**JOSEPH SAMUEL**

*in partial fulfilment of the requirements*
*for the award of the degree of*

**BACHELOR OF TECHNOLOGY**


**DEPARTMENT OF ELECTRICAL ENGINEERING**
**INDIAN INSTITUTE OF TECHNOLOGY MADRAS.**

**June 2016**

# THESIS CERTIFICATE

This is to certify that the thesis titled **Implementation, Evaluation, and Applications of Linearization-based Self-Interference Cancellation for Full Duplex Radios**, submitted by **Joseph Samuel**, to the Indian Institute of Technology, Madras, for the award of the degree of **Bachelor of Technology**, is a bona fide record of the research work done by him under my supervision. The contents of this thesis, in full or in parts, have not been submitted to any other Institute or University for the award of any degree or diploma.

**Prof. Radha Krishna Ganti**
Research Guide
Assistant Professor
Dept. of Electrical Engineering
IIT Madras, 600 036

Place: Chennai

Date: 10th June 2016

# ACKNOWLEDGEMENTS

I thank Prof. Radha Krishna Ganti for being an excellent guide throughout the project. His enthusiasm for the project, as evidenced by him sitting with us debugging the setup numerous times, motivated and inspired me a lot.

I would like to thank Arjun Nadh, with whom I worked together for the most part of my project. His passion for SDRs combined with his PJ skills (which in turn improved mine too) made my BTP days a memorable experience.

I sincerely thank Dr. Klutto Milleth (CEWiT) and Ankit Sharma for their guidance in the Adjacent Channel Interference part of the project. I also thank Prof. S. Aniruddhan and his students Gaurav and Abhishek for their help in RF and circuits portions of the project. I also express my gratitude to Avichal Kulshrestha from National Instruments and the LabVIEW community for their help in LabVIEW programming. I would also like to thank all the members of the Networks and Stochastic Systems Lab for providing a conducive atmosphere for doing research.

Apart from these direct influencers, I would like to thank Prof. David Koilpillai who kindled my interest in wireless communications and the IITMSAT project which gave me my first hands-on experience with radios. Finally I would like to thank God Almighty for his blessings during my stay at IITM; also my family, my friends and members of the St. Gregorios Syrian Orthodox Church, Perumbakkam, for their support.

# ABSTRACT

KEYWORDS: Self-interference cancellation; In-band full duplex; Adjacent Channel Interference; LabVIEW.

Full-duplex wireless communication involves transmitting and receiving at the same time and at the same frequency. A linearization technique to simplify the design of full-duplex radios is presented. The implementation of a prototype of the same is described. The system has an extremely small form-factor compared to current full duplex designs but still gives decent performance. An interesting application of full duplex techniqes in Adjacent Channel Interferece (ACI) cancellation is also demonstrated.

# TABLE OF CONTENTS

# LIST OF FIGURES

# ABBREVIATIONS

| | |
|---|---|
| **OFDM** | Orthogonal Frequency Division Multiplexing |
| **RF** | Radio Frequency |
| **ISM** | Industrial, Scientific and Medical band |
| **LTE** | Long Term Evolution |
| **LNA** | Low Noise Amplifier |
| **ADC** | Analog to Digital Converter |
| **DAC** | Digital to Analog Converter |
| **ACI** | Adjacent Channel Interference |
| **VI** | Virtual Instrument |

# NOTATION

| | |
|---|---|
| $t$ | Time |
| $f$ | Frequency |
| $E(x)$ | Expectation of $x$ |

# CHAPTER 1

# INTRODUCTION TO FULL DUPLEX RADIOS

Full-duplex wireless communication involves transmitting and receiving at the same time and at the same frequency. An ideal full-duplex communication system has double the usable bandwidth in a bi-directional link. However, self-interference is a major impediment in realizing a full-duplex system as the much stronger transmit signal drowns the received signal and in the process saturates the receiver chain.

## 1.1 Origin of self-interference

The signal coming into the receiver of a full duplex system will have not just the intended received signal but also many copies of the transmitted signal coming through various paths. These paths arise because of the following reasons:

1. Transmitter and receiver coupling at the antenna.
2. Leakage of the transmit signal from the power amplifier to the receiver. This can happen via the printed circuit board (PCB) substrate (for a system implemented on a board) or the silicon substrate (for a system implemented on an integrated circuit).
3. Reflections of the transmitted signal from the external environment picked up by the antenna. These reflections are typically attenuated due to path-loss and therefore the strength of the reflected signal depends on the distance to the reflector.

While the self-interference signal components arising out of 1 and 2 can be estimated a priori through calibration, the characteristics of the self-interference paths caused 3 are random and depend on the geometry of the reflectors.

# CHAPTER 2

# PREVIOUS WORK

In current approaches, the self-interference is canceled at multiple stages beginning with the RF stage followed by cancellation in the baseband analog and digital domains. We will now briefly review some of the existing self-interference cancellation techniques.

## 2.1 RF cancellation techniques

In a two antenna system, antenna separation is a simple way of providing passive isolation between the transmit and the receive chains Everett *et al.* (2014); Bliss *et al.* (2007). The isolation depends on the separation distance between antenna, orientation and polarization. In general, the isolation can be upwards of 40 dB. However, in this paper we focus on shared antenna architecture wherein a single antenna is used for both transmission and reception.

In Sahai *et al.* (2011); Duarte and Sabharwal (2010) the entire transmit chain is replicated for generating a duplicate copy of the self-interference signal for cancellation. However, the additional RF chain introduces noise and canceling the non-linearities introduced by the PA in the transmit path is much more difficult. A common technique for RF self-interference cancellation in shared antenna architectures is to use a multitap RF filter with fixed delay lines and tunable gains. In Bharadia *et al.* (2013), sixteen RF delay lines with variable gains were used to filter the known RF signal. The delays (in the range of 400 ps to 1.4 ns) were permanently tuned to the strongest self-interference paths through the PCB and the antenna. An RF cancellation of about 60 dB is reported (in conjunction with a circulator). In Huusari *et al.* (2015), a three-path RF filter using vector modulators is implemented. Also, the control logic of the vector modulators is implemented in the analog domain and an RF cancellation of 60 dB for 20 MHz is reported. This technique of implementing an RF filter (tap-delay line filter) has the following disadvantages:

1. It requires multiple delay lines, and achieving delays at high frequencies in the RF domain is extremely difficult.
2. It is difficult to realise such a multi-tap RF filter in a small form factor.
3. The RF lines have to be carefully tuned a priori and the resulting circuit might not work effectively if the reflectors and the self-interference paths change substantially.

A 35-40 dB passive isolation was reported in Kumar *et al.* (2014); Knox (2012) using hybrid transformers and a vector modulator. An electrical balance tunable RF network was used in van Liempd *et al.* (2014) to provide an isolation of greater than 50 dB in the RF domain with a combination of active and passive techniques.

In summary, the passive isolation techniques (separation of antenna, circulator) can provide about 40 dB isolation Knox (2012), the active cancellation techniques provide about 35-40 dB isolation providing the total RF isolation to be about 65-70 dB for 20 MHz bandwidth.

## 2.2 Baseband analog cancellation

In Kaufman *et al.* (2013), an analog cancellation technique is proposed in conjunction with an antenna design. However, the gains of the analog cancellation in isolation are not clear. Analog cancellation techniques while recognized as important, are not common because of the restricted access to the baseband signals in commercial off-the-shelf (COTS) equipment.

## 2.3 Baseband digital cancellation

Digital baseband cancellation consists of removing the residual self-interference after RF and baseband analog cancellation. In Bharadia *et al.* (2013); Duarte and Sabharwal (2010), the SI channel is estimated Bharadia *et al.* (2013) using a least-squares technique and the SI is cancelled using the estimated channel and the known transmitted signal. However, these techniques incur significant complexity since the entire channel (with unknown number of taps) has to be estimated constantly to track the

channel changes due to the varying reflections. The importance of removing the non-linear components of the signal are highlighted in Bharadia *et al.* (2013) and $45$ dB digital cancellation was reported. Other implementations Duarte and Sabharwal (2010) have reported about $30$ dB cancellation. In Day *et al.* (2012), it has been shown that the limited dynamic range of the analog-to-digital conversion is a bottleneck in effective cancellation of self-interference in the digital domain. In Choi and Shirani-Mehr (2013), the system level performance of full-duplex radios is presented. In all these digital techniques, no prior model of the filter (for the linear components) is used leading to a higher implementation complexity. Digital cancellation leads to about 35-40 dB of self-interference suppression for most of these designs.

# CHAPTER 3

# BASIC IDEA: LINEARIZATION

We now introduce the technique of linearization of the self-interference signal that would form the basis of our new cancellation technique.

## 3.1 First order approximation

We use a first order Taylor series approximation for the delayed signal $x(t-\tau_k)$ to obtain

$$x(t-\tau_k) = x(t) - x'(t)\tau_k + E(\tau_k, t), \tag{3.1}$$

where $E(\tau_k, t)$ is the residual error, and $x'(t) = \frac{dx(t)}{dt}$ is the derivative of the baseband signal. The error term decreases with decreasing $\tau_k$ improving the approximation. We will now express the self-interference signal as a function of the baseband signal $x(t)$ and its derivatives. We have

$$\begin{aligned}
I(t) &= \sqrt{G_t}\sum_{k=1}^{M} a_k \Re[x(t-\tau_k)e^{j2\pi f_c(t-\tau_k)}] \\
&\overset{(a)}{=} \sqrt{G_t}\sum_{k=1}^{M} a_k \Re[(x(t) - x'(t)\tau_k + E(\tau_k,t))e^{j2\pi f_c(t-\tau_k)}] \\
&= \sqrt{G_t}\Re\Big[\sum_{k=1}^{M} a_k x(t)e^{j2\pi f_c t}e^{-j2\pi f_c\tau_k} - \\
&\qquad\qquad \sum_{k=1}^{M} a_k x'(t)\tau_k e^{j2\pi f_c t}e^{-j2\pi f_c\tau_k}\Big] + E_2(t) \\
&= \sqrt{G_t}\Re\Big[x(t)e^{j2\pi f_c t}C_0 - x'(t)e^{j2\pi f_c t}C_1\Big] + E_2(t),
\end{aligned}$$

where

$$C_0 = \sum_{k=1}^{M} a_k e^{-j2\pi f_c\tau_k},$$

and

$$C_1 = \sum_{k=1}^{M} a_k \tau_k e^{-j2\pi f_c \tau_k}.$$

Here $(a)$ follows from (3.1) and $E_2(t)$ is the error term given by

$$E_2(t) = \sqrt{G_t} \sum_{k=1}^{M} a_k \Re[E(\tau_k, t) e^{j2\pi f_c (t-\tau_k)}]. \tag{3.2}$$

In the above expression, observe that $C_0$ and $C_1$ are complex numbers that are constant (for a given geometry of backscatters) and depend only on the path-loss and the path delays. Hence the self-interference can be expressed as

$$I(t) = I_s(t) - I_d(t) + E_2(t), \tag{3.3}$$

where $I_s(t) = \Re[C_0 x(t) e^{j2\pi f_c t}]$, represents the self-interference because of the signal and $I_d(t) = \Re[C_1 x'(t) e^{j2\pi f_c t}]$ represents the self-interference because of the derivative term. If the error term $E_2(t)$ is small, canceling $I(t)$ would amount to canceling the interference because of $I_s(t)$ and $I_d(t)$ which only depend on the signal $x(t)$ and its derivative $x'(t)$. In other words, we do not require to construct many different delayed copies of $x(t)$ to cancel the self-interference signal – we just need the signal $x(t)$ and its derivative $x'(t)$. The signal $x(t)$ is readily available in the analog domain since that is the signal being transmitted. The derivative $x'(t)$ can easily be generated in the analog or digital domain (which will be explained in the next Section).

Neglecting $E_2(t)$, the channel can now be modelled as $H(f) = C_0 + C_1 f$. The effect of the entire channel is now captured by just two complex numbers $C_0$ and $C_1$, thus providing a huge dimensionality reduction – the number of parameters to estimate is only two irrespective of the nature and number of multipaths.

The Taylor series is a good approximation for paths arising with low $\tau_k$ and the error is large for paths with large $\tau_k$. However, paths with large $\tau_k$ arise from far-off reflectors and hence the path loss for these paths is large, and therefore the absolute error contribution by these paths is low. Hence the overall approximation of $I_t$ by $I_s$ and $I_d$ is reasonable for signals with low bandwidth. We will make this observation precise in the next Lemma by bounding the power of the error.

# CHAPTER 4

# IMPLEMENTATION – SETUP

## 4.1 Overview

A significant part of the self-interference signal should be cancelled before the LNA to prevent saturation and non-linearities in various elements of the receiver chain. Cancelling a part of the SI signal in the RF domain also helps in suppressing the in-band transmitter noise. So the larger component $I_s(t)$ of the self-interference term has to be cancelled before the LNA. The derivative signal can be cancelled either in the RF domain (before LNA), or in the analog baseband domain (before Analog to Digital Converter (ADC) and after mixer) or in the digital baseband domain (after ADC). These three options lead to three different architectures. However, as a proof of concept and for ease of implementation, we cancel the derivative term in the digital domain.

## 4.2 Experimental Setup

Our experimental setup is shown in Fig. 4.2. We use a National Instruments (NI) PXIe based software defined radio (NI5791) for transmission and reception. The maximum transmit power possible in NI5791 is 5 dBm and we use an external power amplifier (PA) (Skyworks SE2576L) at the transmitter. We use a shared antenna architecture wherein the same antenna is used for transmission and reception. The isolation between transmit and receive chain is provided by a circulator (Pasternack PE8401). This circulator provides 18 dB of isolation between port 1 and port 3. The transmit signal is fed into port 1 and the antenna is connected to port 2. The signal from port 3 will therefore contain the received signal as well as the self-interference signal. Two copies of the transmit signal from PA are obtained using a directional coupler (Mini-Circuits ZHDC-16-63-S+), wherein one is connected to the input port of the circulator and the other is used as an input to the vector modulator (Hittite HMC631LP3). The directional coupler allows for tapping a copy of a signal with minimal loss in the mainline, thus the output

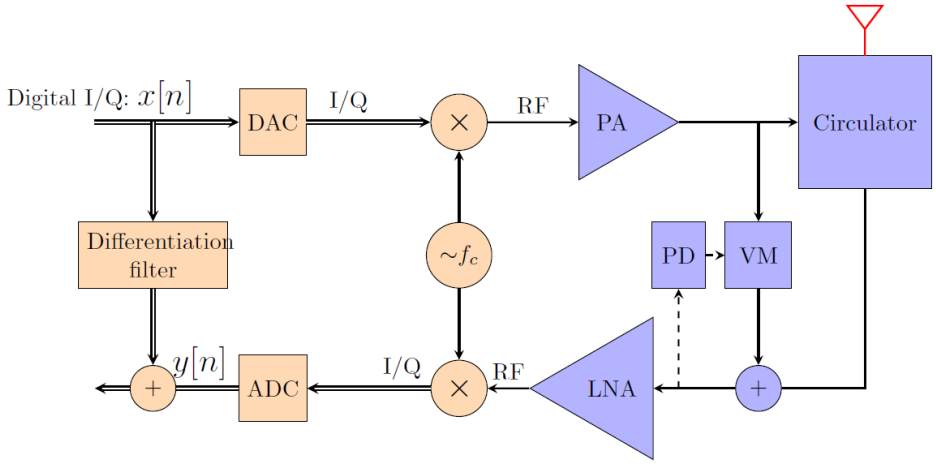


Figure 4.1: Self-interference cancellation architecture.

at the coupled port is much lower in power[1]. The VM also introduces an attenuation and thus the power at its output may be insufficient to suppress the self-interference. The output of VM is passed through an amplifier (Mini-Circuits ZX60-P33ULN+) in order to recover this loss in power. The self-interference signal at port 3 of the circulator is comprised of the transmit signal leaked through the circulator and multiple reflected copies of the transmit signal received by the antenna.

As mentioned earlier, the signal component ($I_s(t)$) of the self-interference is cancelled in the RF domain. The vector modulator is used to adapt the gain and phase of the tapped transmitted signal and match it to the $I_s(t)$ component of the self-interference. The gain and phase of the VM are controlled by two DC voltages generated by an NI Data Acquisition Device (DAQ)[2]. The output of the VM and the self-interference signal (from the receive port of the circulator) are summed by a power combiner (Mini-Circuits ZX10-2-232-S+). A part of this summed signal is fed to a true RMS power detector (PD) (Hittite HMC1020LP4ETR) via a power splitter to observe the power in the residual signal. The PD generates a DC voltage proportional to the input power. This voltage is sampled by the NI DAQ. The optimal DC control voltages of the VM are found by an adaptive search that minimizes the residual self-interference power.

[1] A lower power at the input of the VM is desirable since the P1 dB of the VM that we use is 21 dBm and a lower power at its input prevents any significant non-linearity at the output of the VM.

[2] Consists of 16-bit analog-to-digital converters (ADC) and 16-bit digital-to-analog converters (DAC) controllable by a desktop computer

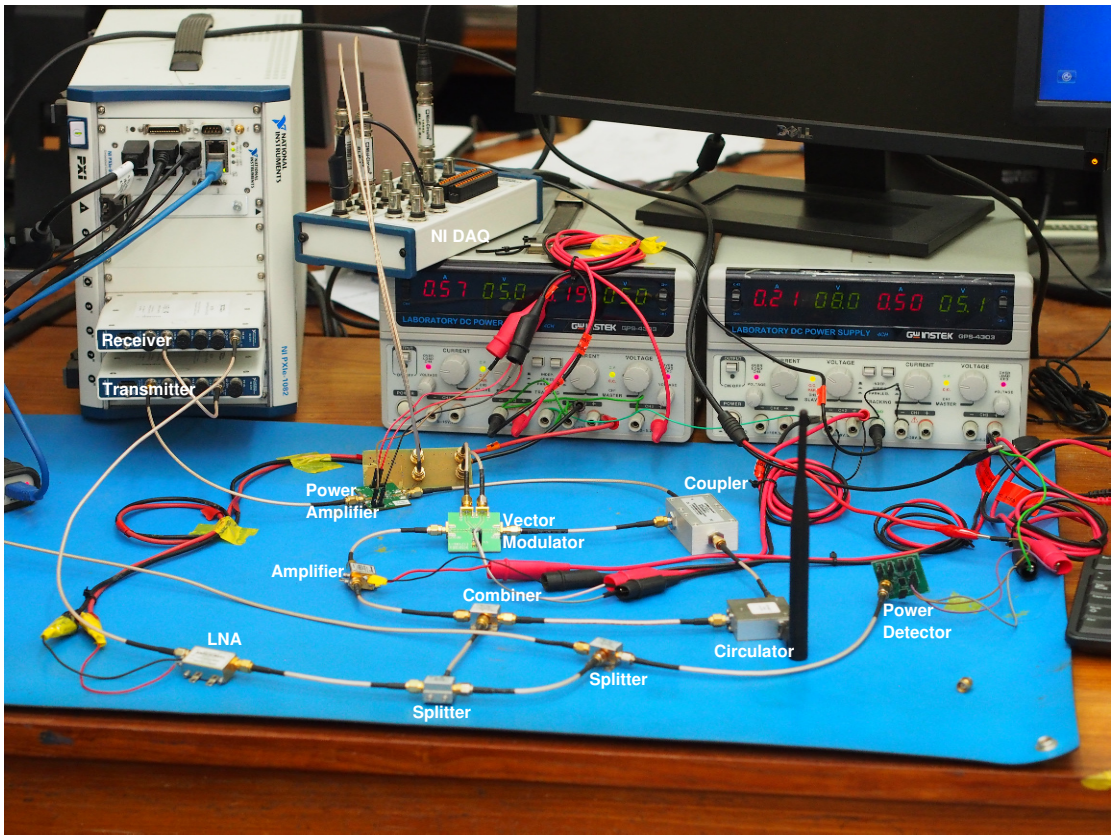


Figure 4.2: Experiment Setup

The residual signal after the combiner is fed to the NI5791 receiver[3]. The received samples comprise of the signal term and the derivative term. A part of these samples are training symbols. They are processed offline to obtain $\hat{a_0}$, $\hat{c_1}$ and $\hat{c_2}$. These estimated parameters are then used to reconstruct and cancel self-interference for the remaining samples. (Non-linear cancellation of the third and fifth harmonic is also used to mitigate the non-linear effects of the PA.)

[3]The minimum RF power at the input of 5791, that induces full-scale swing at the ADC is -27 dBm. Since the residual self-interference signal is much lower in power, we use an (Mini-Circuits ZX60-242GLN-S+) before the NI5791 module, to prevent effect of quantization noise.

# CHAPTER 5

# IMPLEMENTATION – ADAPTIVE ANALOG CANCELLATION

## 5.1 Motivation

Currently, the optimum gain and phase values of the Vector Modulator was being found out using a brute force grid search. The search takes many seconds to about a minute to complete, depending on the resolution of the search grid. Now, this is a problem when the channel changes in the actual scenario. It is not possible to run the algorithm all over again. Therefore some kind of adaptive technique is warranted to adjust the gain and phase values according to the changing channel conditions.

## 5.2 Technique

The following simple technique was used: the brute force algorithm is run initially when the system starts. This algorithm gives a particular gain and phase value. Let them be $G_0$ and $\theta_0$ respectively. Now, after $T_u$ seconds, the setup changes gain and phase to the 9 values $(G, \theta) = (G_0 + k\Delta, \theta_0 + k\Delta),\ k = -1, 0, 1$. It then checks for which of these 9 coordinates give the minimum received power and switches to the corresponding $(G, \theta)$. This adaptive search is repeated again after $T_u$ seconds.

$T_u$ and $\Delta$ are parameters of the algorithm.

## 5.3 Implementation in LabVIEW

The above technique was implemented in LabVIEW and was interfaced with the DAQ board and power detector. Figure 5.1 shows controls and indicators of the algorithm on the LabVIEW VI Front Panel.

This technique was verified to be working with the actual setup even under stressful conditions – the antenna orientation was changed suddenly but still the algorithm could recalculate the new optimal $(G, \theta)$ point.

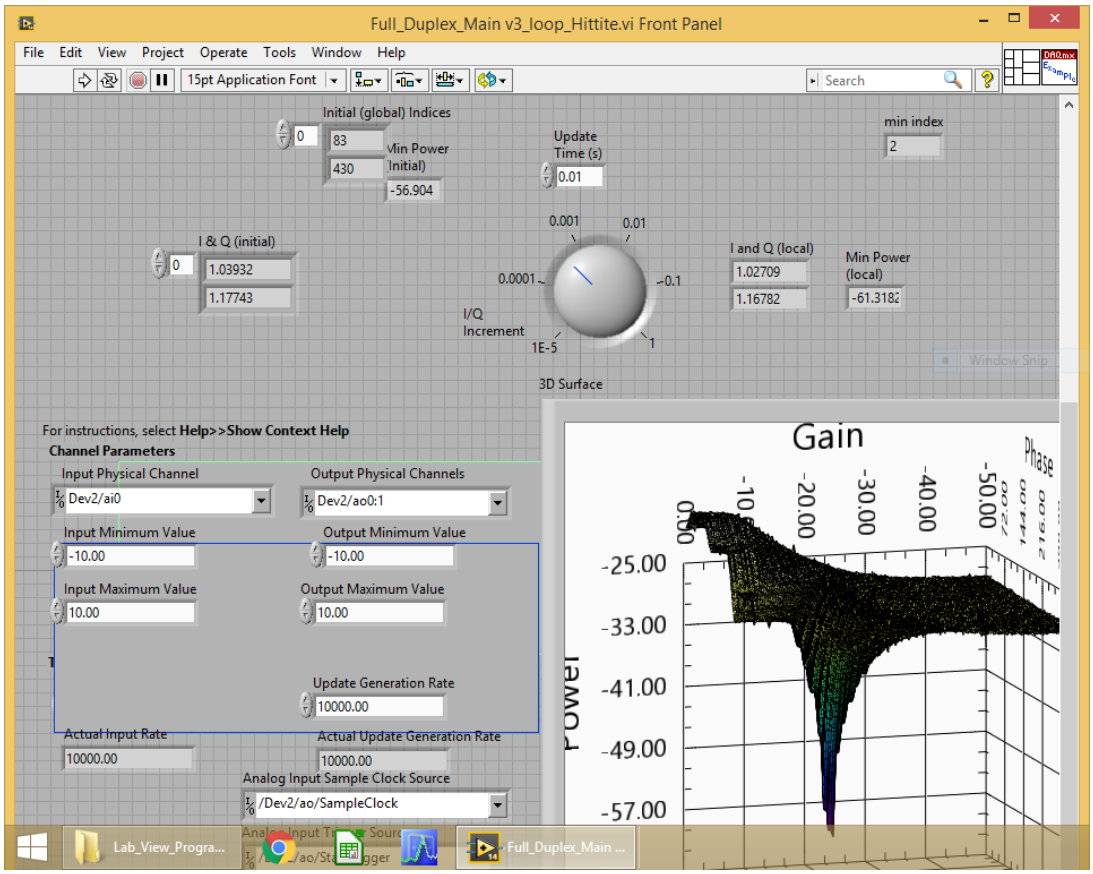


Figure 5.1: Controls and indicators of the adaptive algorithm on the LabVIEW VI Front Panel.

# CHAPTER 6

# IMPLEMENTATION – REAL-TIME IMPLEMENTATION

## 6.1 Real-time Implementation in PC

The above setup cannot be run in real-time on a PC at high bandwidths due to the amount of computations involved. We could successfully run real-time at bandwidths of 1 MHz but not beyond that.

### 6.1.1 Limitations

Since the bandwidths of interest in modern wireless systems can be of the order of 10s of MHz, 1 MHz real-time system was decided not to be sufficient.

## 6.2 Real-time implementation in FPGA

Since we could not go beyond 1 Msps in PC, we decided to implement the algorithm on the FPGA. The implementation is nearing completion.

# CHAPTER 7

# EVALUATION

We obtain the cancellation results for OFDM and single-carrier modulated waveforms.

## 7.1 Waveforms used

### OFDM

We consider an OFDM signal with 1024 subcarriers of which 620 are useful subcarriers (the rest are nulled out at the DC and at the edge of the band). At the receiver we use an oversampling factor of 4. The maximum sampling rate that can be practically achieved using PXIe is 80 MS/s. Hence with an oversampling factor of 4, the maximum bandwidth of OFDM signal that can be transmitted is 20 MHz. The P1dB of the PA is 32 dBm. The measured PAPR (Peak to Average Power Ratio) of the transmitted OFDM waveform was 13 dB and hence the maximum average transmit power was restricted to 19 dBm to avoid severe non-linearities. The spectrum of a 20 MHz OFDM signal that is used is plotted in Figure 7.1.

### Single-carrier

A 4-QAM single-carrier signal was also used for the experiments. An RRC pulse shaping filter with roll-off factor 0.3 was used. The PAPR of the signal was measured to be 4 dB which is about 9 dB lower than that of OFDM. Hence, with the same PA, the single carrier can be transmitted with about 9 dB higher power than OFDM without PA saturation.

We use 2.395 GHz as the center frequency for all the experiments. This was done mainly to avoid interference from the ISM band.

## 7.2 Results and discussion

Following the standard convention in literature, we define cancellation to be ratio of power of the SI signal after cancellation to the power of the SI signal before cancellation. The ratio is expressed in dB. Note that the power of the SI signal before cancellation is the same as transmit power at the antenna port (port 2) of the circulator.

In Figure 7.1, the spectrum of the self-interference signal is plotted when an OFDM signal is transmitted at 4 dBm (at port 2 of the circulator). In the same figure, the residual self-interference is plotted after analog cancellation. About 54 dB of self-interference was cancelled in the analog domain. More importantly, the linear slope in the residual self-interference spectrum indicates that the residual signal is dominated by the derivative component $I_d(t)$, thus verifying the derivative approximation and in particular (3.3).

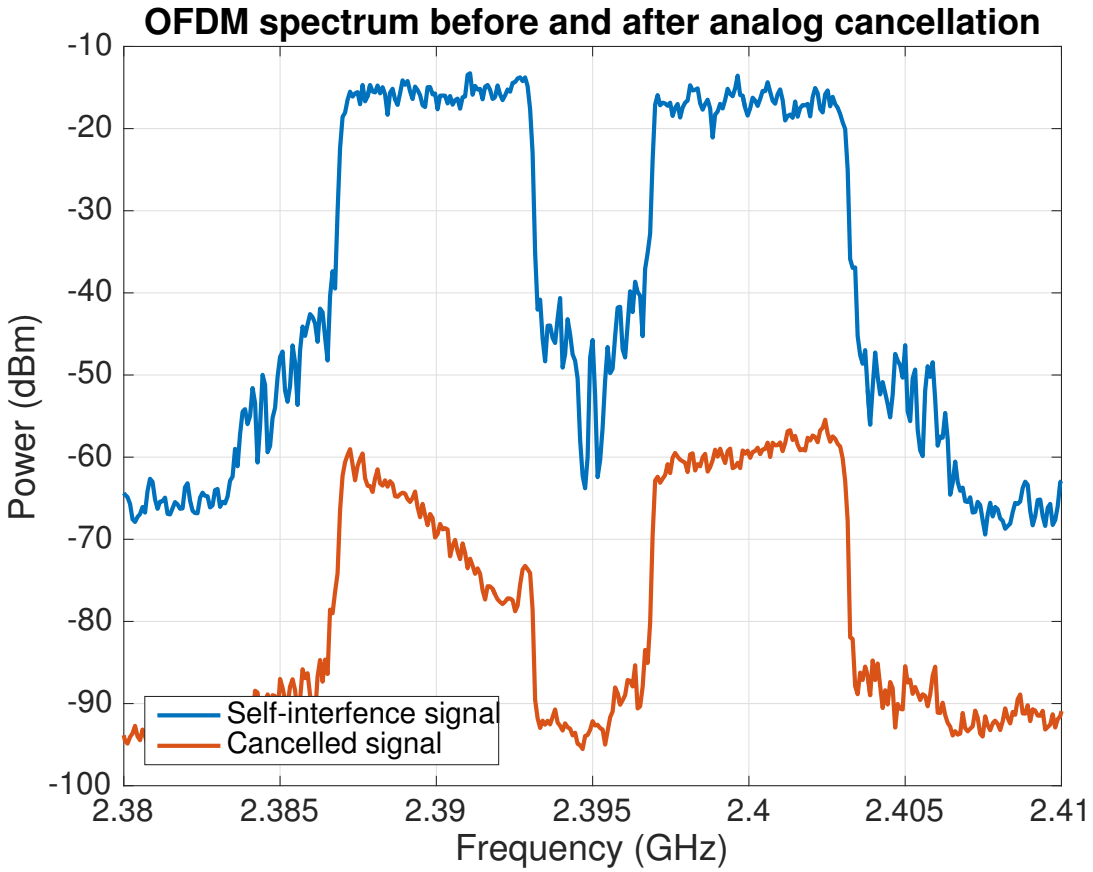


Figure 7.1: The spectrum of the self-interference signal of a 20 MHz OFDM transmission. Also, the self-interference spectrum after analog cancellation is plotted. The transmit power (at the antenna port) is 4 dBm and the analog cancellation is about 54 dB. The linear slope in the residual self-interference indicates a derivative component.

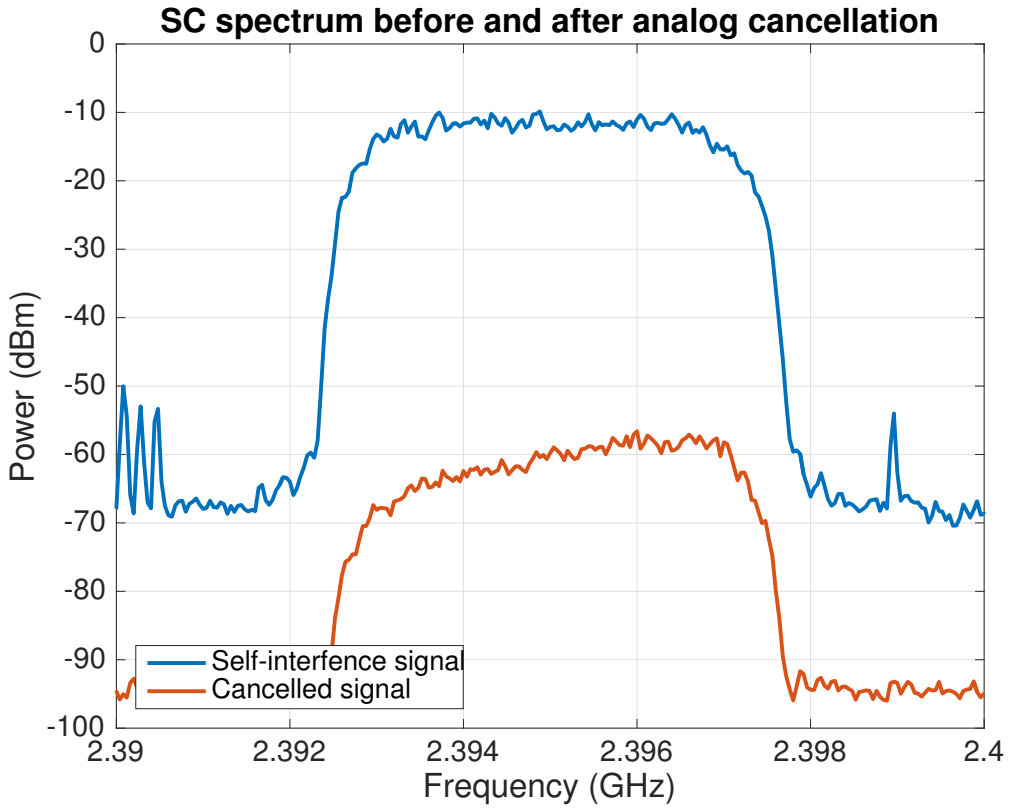


Figure 7.2: The spectrum of the self-interference and the residual signal of a 10 MHz 4-QAM single carrier transmission. The transmit power (at the antenna port) is 4 dBm and the analog cancellation is about 57 dB. The linear slope in the residual self-interference indicates a derivative component.

In Figure 7.2, the spectra of the self-interference and the cancelled signal (57 dB analog cancellation) are plotted when a single-carrier signal is transmitted. As in the OFDM signal, the residual self-interference exhibits a large derivative component.

In Figure 7.3, the analog cancellation[1] is plotted as a function of the signal bandwidth. We observe that the analog cancellation decreases with increasing bandwidth. This is because the derivative component in the residual self-interference signal increases with increasing bandwidth. Since analog cancellation only removes $I_s(t)$, the residual power increases with increasing bandwidth, and thus lowering the analog cancellation. The top curve in the plot corresponds to the case when the antenna port was terminated by a 50 $\Omega$ terminator, while the bottom curve corresponds to measurements with an antenna. In the case of 50 $\Omega$ termination, the self-interference multi-path is primarily through the circulator, while with antenna, there will be multiple paths due to reflections too. In addition, the characteristic impedance of the antenna will not be as close to 50 $\Omega$ as a terminator. This impedance mismatch causes RF signals to get

[1]The reported analog cancellation also includes the 18 dB isolation of the circulator.

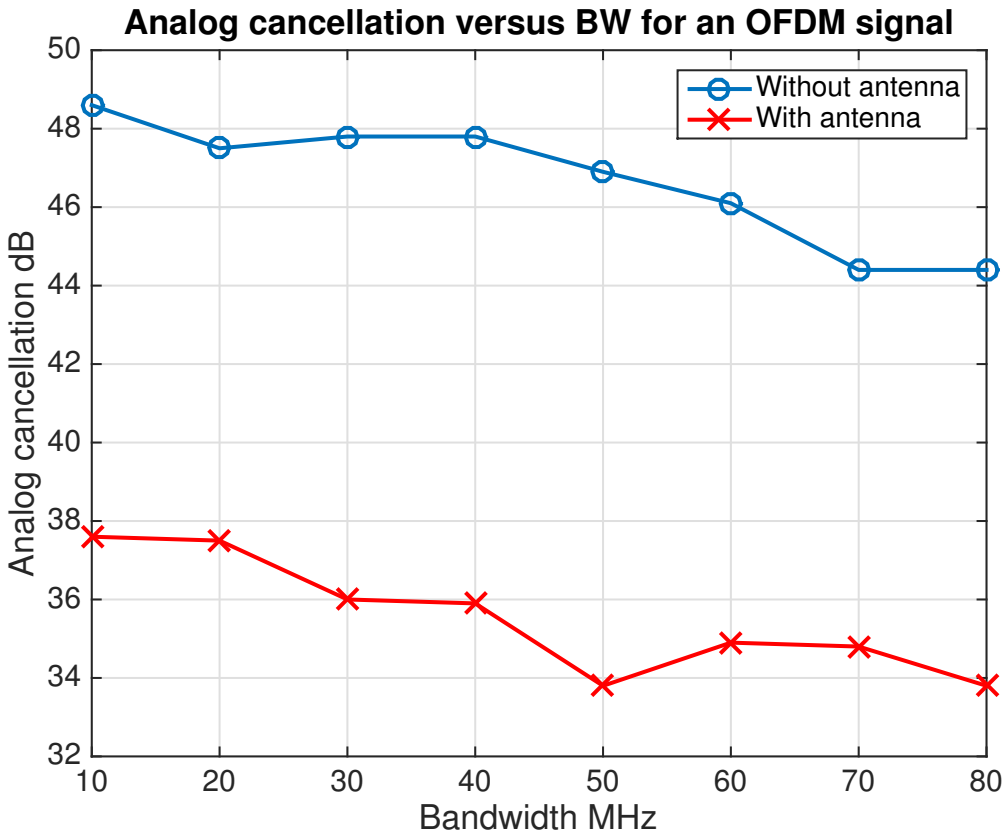


Figure 7.3: Analog cancellation versus transmit BW for an OFDM signal with and without antenna. In the second case (without antenna), the antenna port is terminated by a 50 $\Omega$ terminator.

reflected back from the antenna (instead of getting transmitted). Because of these two effects, the aggregate power in the derivative component increases in the case of antenna. This reduces causes the reduction in analog cancellation.

In Figure 7.4, the analog and digital cancellation are plotted as a function of the transmit power. We observe that the analog cancellation is almost constant with respect to increasing transmit power. This is expected since the analog cancellation does not depend on the signal SNR and depends only on the resolution of the phase and amplitude of the VM, which are fixed. The digital cancellation is increasing with the transmit power till about 5 dBm input power after which it reduces. This is mainly because of the power amplifier non-linearities.

As mentioned earlier, the digital cancellation consists of removing the signal, the derivative and the second order derivative components. In Figure 7.5, this split-up is provided as a function of the transmit power. We see that the first-derivative cancellation provides the maximum cancellation. However, the second-derivative also gives about 5-6 dB of cancellation. The self-interference after analog cancellation is $I(t) = I_s(t) +$

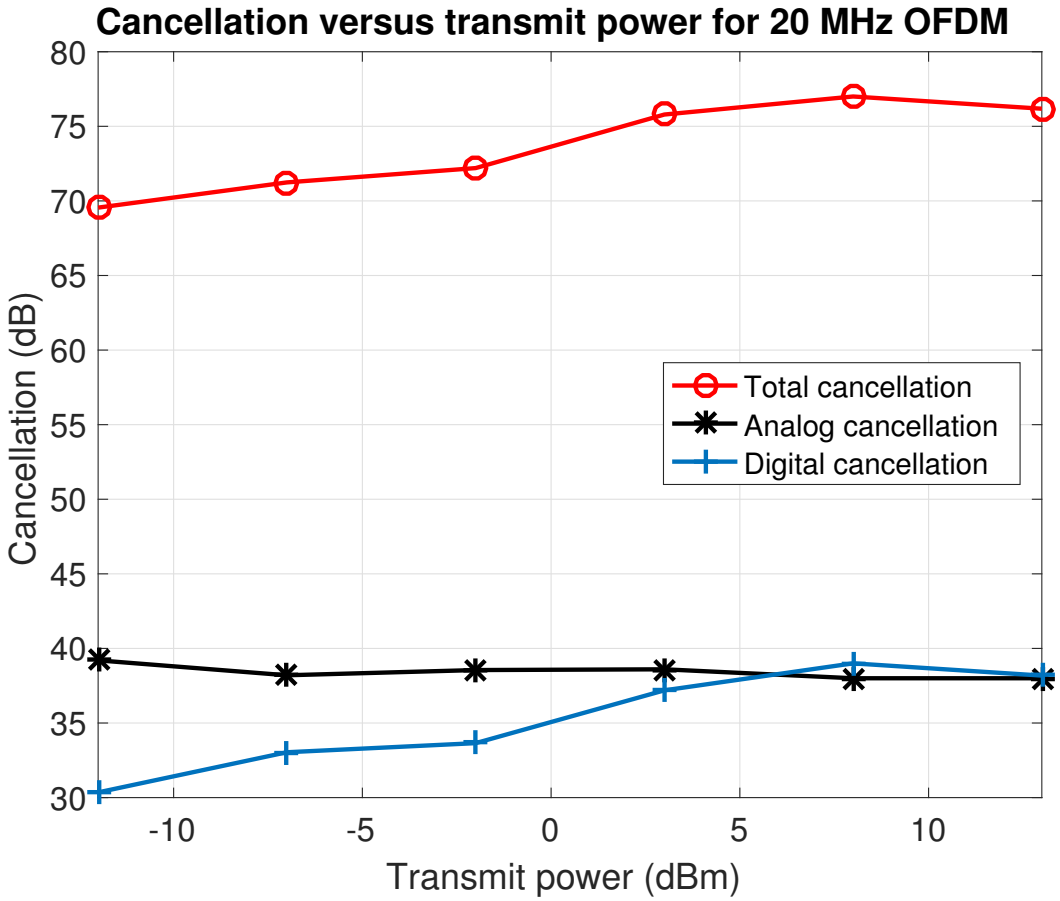


Figure 7.4: Analog and digital cancellation versus transmit power for a 20 MHz OFDM signal with antenna.

$I_d(t)$, *i.e.*, a sum of the the signal and the derivative terms. This signal is received in the digital domain after sampling by the ADC. Since the initial phase of the sampling time cannot be controlled, the received self-interference in the digital domain is $I(nT + \delta) = I_s(nT + \delta) + I_d(nT + \delta)$, $n = 1, 2, \ldots$, where $T$ is the sampling duration and $0 \leq \delta \leq T$. However we only have access to the transmitted signal $x(nT)$. Since $\delta$ is small, $I_s(nT + \delta) = a_0 x(nT + \delta)$ can be approximated (after appropriate scaling by $a_0$) by $x(nT)$ and $x'(nT)$. Similarly $I_d(nT + \delta) = c_1 x'(nT + \delta)$ can be approximated by $x'(nT)$ and the second derivative $x''(nT)$. Hence using the second derivative improves the overall cancellation.

For a single carrier transmission, the cancellation is plotted as a function of the transmitted power in Fig. 7.6. Overall, we observe about 75 dBm cancellation for both OFDM and single-carrier waveforms. Thus the overall cancellation is impervious to the transmitted waveform.

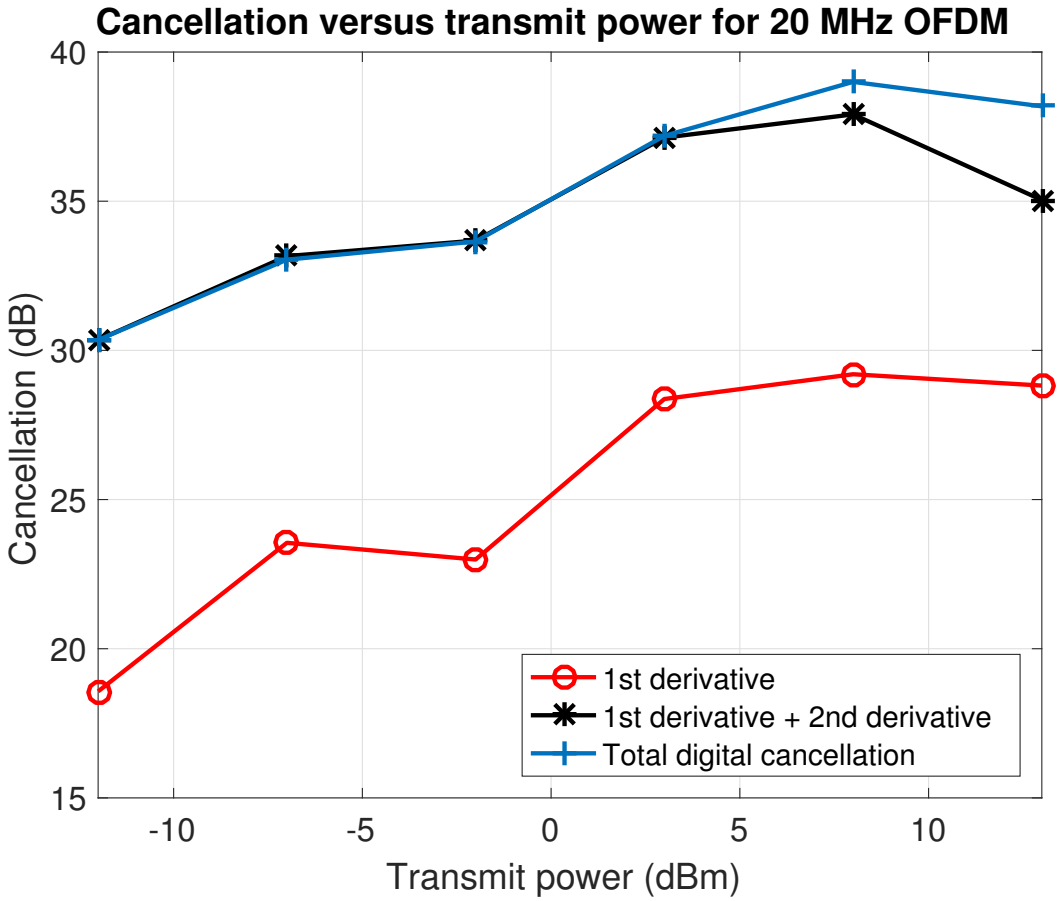


Figure 7.5: Split-up of the digital cancellation versus transmit power for a 20 MHz OFDM signal with antenna.

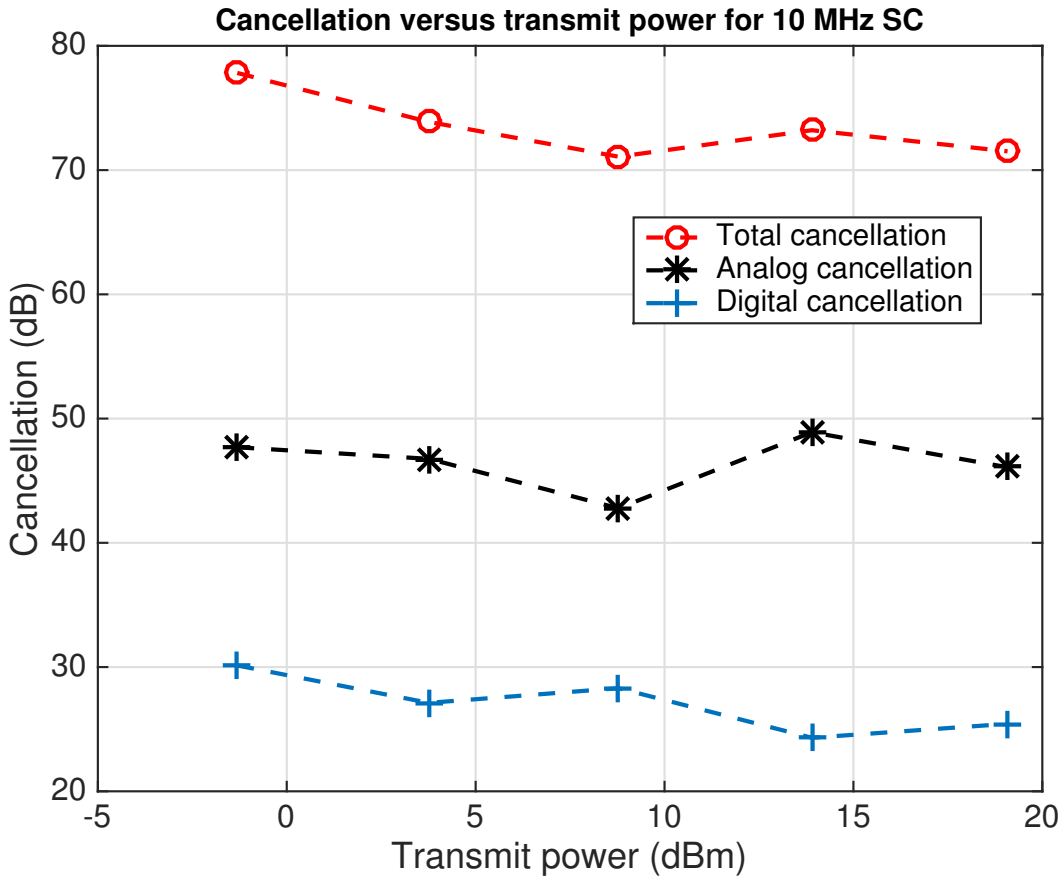


Figure 7.6: Cancellation vs Transmit power for different bandwidths with single carrier as transmit waveform. These results were obtained with port 2 of the circulator connected to an antenna.

# CHAPTER 8

# APPLICATION – ADJACENT CHANNEL INTERFERENCE CANCELLATION

In this chapter, we look at a potential application of self-interference cancellation for applications other than full-duplex communication. We look at its application in adjacent channel interference (ACI) cancellation.

## 8.1 Adjacent Channel Interference

Adjacent channel interference is a major challenge in LTE base stations. Consider two operators A and B operating on neighbouring channels from the same physical base station. Assume that A is transmitting and B is receiving in adjacent channels. The high power transmit from A will swamp out B's receiver. This is called Adjcent Channel Interference or ACI.

### 8.1.1 Current approaches to reduce ACI

To mitigate this problem, two approaches (which are often combined) are used

1. Give guard bands between channels. However, this leads to wastage of spectrum.
2. Use high-Q filters to avoid out-of-band emissions. However, high-Q filters are very costly.

## 8.2 Using full-duplex techniques to mitigate ACI

We demonstrate that full-duplex techniques can be used to reduce ACI in a more efficient and cost-effective manner.

The problem of ACI is similar to the normal full-duplex problem in the sense that a high power transmission is interfering with reception at low powers. However, there are two major differences

- The interfering transmitter is not the same device as the receiver – it is from a different equipment. In our example above, B is getting interference from the transmission of A and not B itself.
- The interference is not in the same band/channel in which you are trying to receive. It is from the adjacent band.

These two differences do not cause hindrance to the analog cancellation architecture so long the receiver has access to the interfering RF signal. We assume the latter. The assumption is perfectly valid because all LTE transmissions are encrypted and operator A should not have any issues in sharing its RF signal with operator B.

## 8.3 Setup and Procedure

We demonstrate ACI cancellation using full duplex using a prototype setup. The setup used is shown in Figure 8.1.

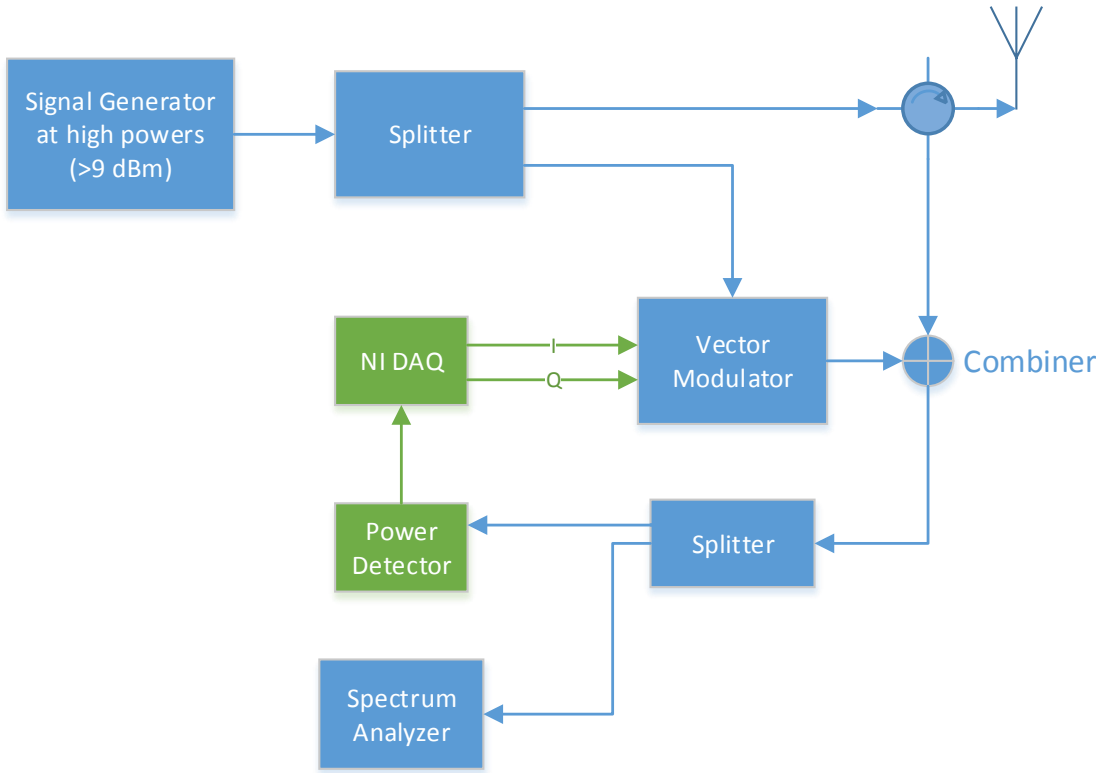


Figure 8.1: Block diagram of setup for ACI cancellation demonstration.

The setup used is shown in Figure 8.1. The signal generator transmits at powers high enough to produce sufficient out-of-band emissions.

**Step 1 – Power without cancellation**

First, the interfering transmitter power was measured at the point after the circulator. The signal generator transmits a 5 MHz OFDM signal.

**Step 2 – Tuning**

The setup was then tuned by sending a sinusoid and noting the magnitude and phase which gives the maximum cancellation at the input of the power detector.

**Step 3 – Power after Cancellation**

Once tuning was done, the signal generator is made to transmit the 5 MHz OFDM signal again. The power of the cancelled signal is measured at the output of the combiner. The difference (in dB) between the powers in Step 1 and Step 3 at different frequencies in the adjacent channel is calculated. Note that this figure will give an extra 3 dB because Step 1 measurement is taken at the output of the circulator while the Step 3 measurement is taken after the combiner.

## 8.4 Results

### 8.4.1 Cancellation at different individual out-of-band frequencies

The cancellation at four different frequency points in the band were calculated – at a distance of 2.5, 3, 5 and 8 MHz from the center frequency. This was done for transmit powers of 9 dBm, 11 dBm, 13 dBm and 15 dBm. There were no significant out-of-band emission below 9 dBm.

Screenshots of the spectra before and after cancellation for 15 dBm transmit power are shown in Figures 8.2 and 8.3 respectively. The 4 frequency points under consideration are the ones corresponding to markers M1 to M4.

The cancellation at the four frequency points for different transmit powers can be summarized as shown in Figure 8.4.

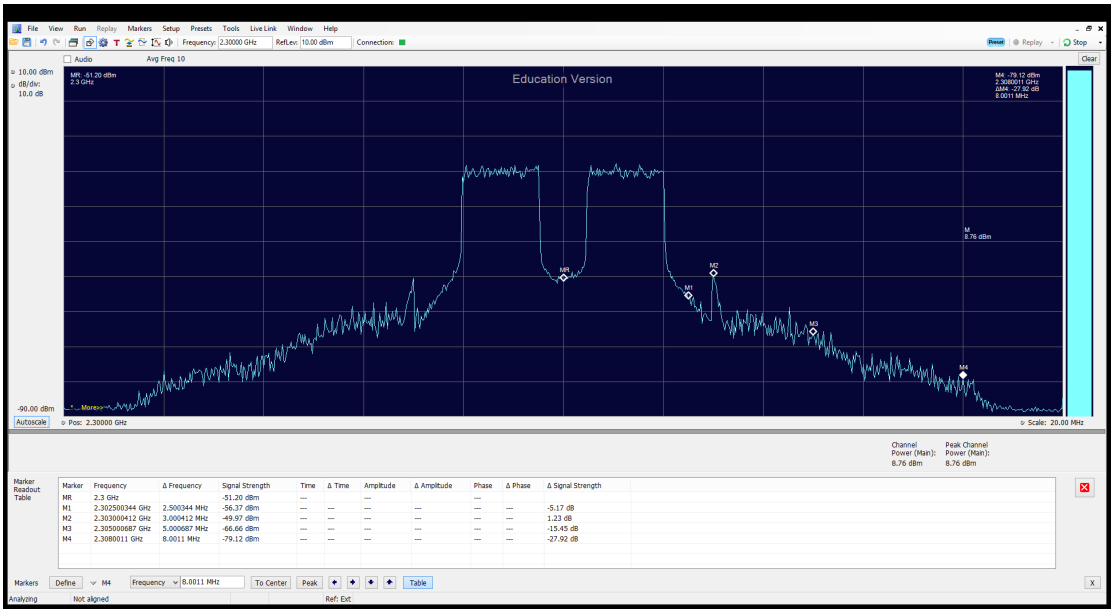


Figure 8.2: Spectrum before cancellation for 15 dBm transmit power.

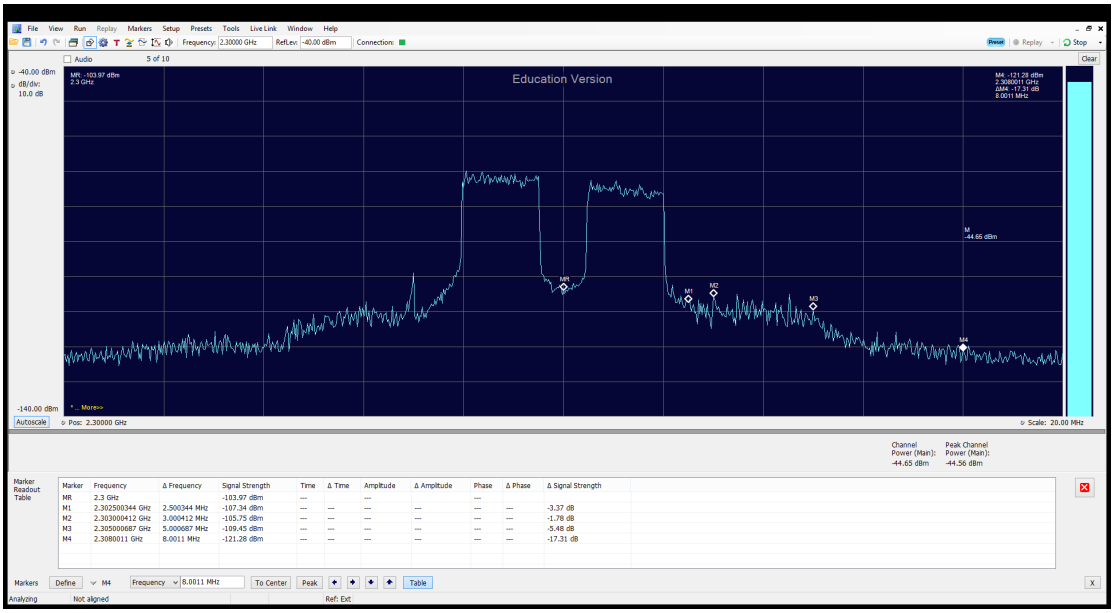


Figure 8.3: Spectrum after cancellation for 15 dBm transmit power.

It can be seen that about 40 dB of cancellation can be achieved using analog methods alone.

### 8.4.2 Cancellation in the adjacent 5 MHz band

The integrated power in the adjacent 5 MHz band was also calculated. The amount of cancellation using this metric comes out to be about 45 dB. The variation with transmit power is shown in Figure 8.5.

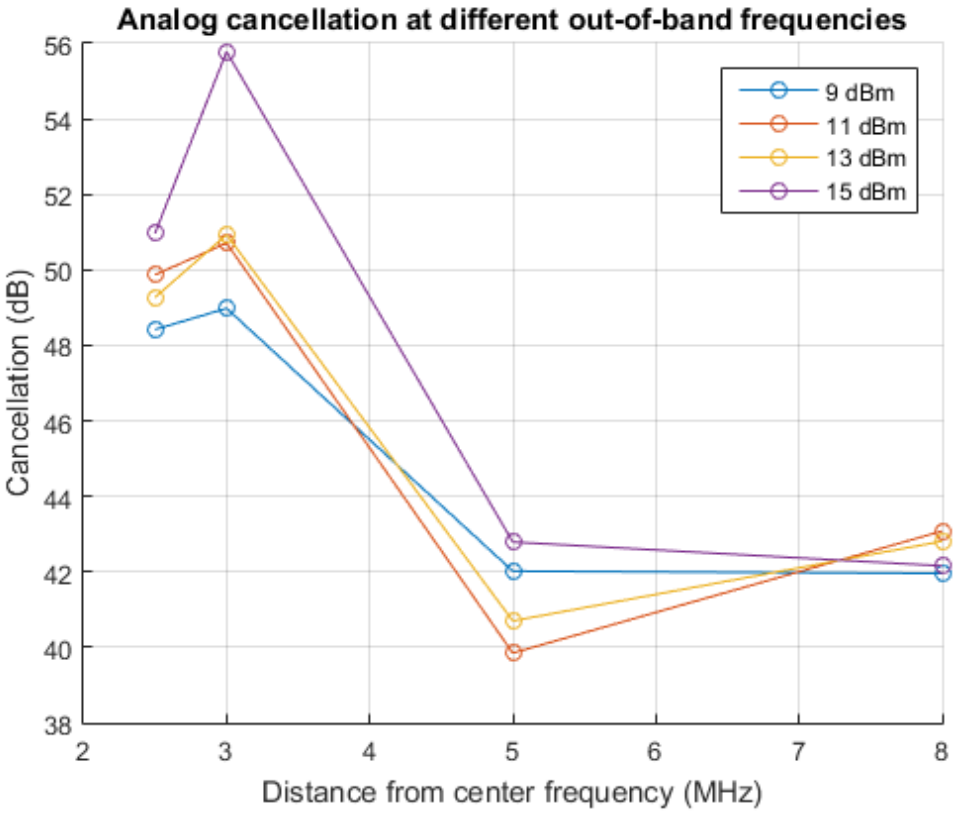


Figure 8.4: Cancellation at different out-of-band frequencies.

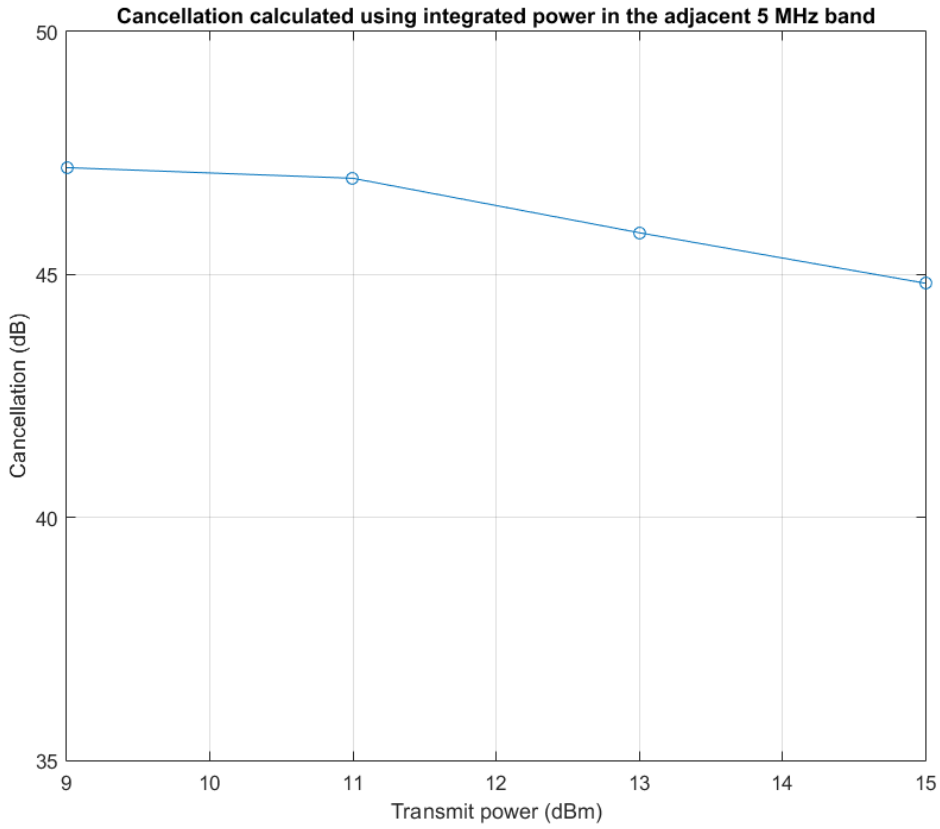


Figure 8.5: Cancellation calculated by using the integrated power in the adjacent 5 MHz band.

# CHAPTER 9

# CONCLUSION AND FUTURE WORKS

This thesis presented an overview of linearization technique for full-duplex radios and some of its applications. Since linearization approximation allows for much smaller form-factors, this idea can lead to widespread adoption of full-duplex radios.

## 9.1 Possible Future Works

Here are the some of the possible avenues for future researchers in this area:

- Exploration onto why non-linear cancellation is not giving good results.
- Using two vector modulators in the cancellation setup.
- More research into ACI Cancellation application. A direct side-by-side comparison with an actual high-Q filter could be made.

# REFERENCES


1. **Bharadia, D.**, **E. McMilin**, and **S. Katti**, Full duplex radios. *In Proceedings of the ACM SIGCOMM 2013 conference on SIGCOMM*. ACM, 2013.

2. **Bliss, D. W.**, **P. A. Parker**, and **A. R. Margetts**, Simultaneous transmission and reception for improved wireless network performance. *In 2007 IEEE/SP 14th Workshop on Statistical Signal Processing*. 2007.

3. **Choi, Y.-S.** and **H. Shirani-Mehr** (2013). Simultaneous transmission and reception: Algorithm, design and system level performance. *Wireless Communications, IEEE Transactions on*, **12**(12), 5992–6010. ISSN 1536-1276.

4. **Day, B. P.**, **A. R. Margetts**, **D. W. Bliss**, and **P. Schniter** (2012). Full-duplex MIMO relaying: Achievable rates under limited dynamic range. *Selected Areas in Communications, IEEE Journal on*, **30**(8), 1541–1553.

5. **Duarte, M.** and **A. Sabharwal**, Full-duplex wireless communications using off-the-shelf radios: Feasibility and first results. *In Signals, Systems and Computers (ASILOMAR), 2010 Conference Record of the Forty Fourth Asilomar Conference on*. IEEE, 2010.

6. **Everett, E.**, **A. Sahai**, and **A. Sabharwal** (2014). Passive self-interference suppression for full-duplex infrastructure nodes. *IEEE Transactions on Wireless Communications*, **13**(2), 680–694. ISSN 1536-1276.

7. **Huusari, T.**, **Y.-S. Choi**, **P. Liikkanen**, **D. Korpi**, **S. Talwar**, and **M. Valkama**, Wideband self-adaptive RF cancellation circuit for full-duplex radio: Operating principle and measurements. *In Vehicular Technology Conference (VTC Spring), 2015 IEEE 81st*. 2015.

8. **Kaufman, B.**, **J. Lilleberg**, and **B. Aazhang**, An analog baseband approach for designing full-duplex radios. *In Signals, Systems and Computers, 2013 Asilomar Conference on*. IEEE, 2013.

9. **Knox, M. E.**, Single antenna full duplex communications using a common carrier. *In Wireless and Microwave Technology Conference (WAMICON), 2012 IEEE 13th Annual*. IEEE, 2012.

10. **Kumar, A.**, **S. Aniruddhan**, and **R. K. Ganti**, Directional coupler with high isolation bandwidth using electrical balance. *In Microwave Symposium (IMS), 2014 IEEE MTT-S International*. IEEE, 2014.

11. **Sahai, A.**, **G. Patel**, and **A. Sabharwal** (2011). Pushing the limits of full-duplex: Design and real-time implementation. *CoRR*, **abs/1107.0607**. URL `http://arxiv.org/abs/1107.0607`.

12. **van Liempd, B.**, **B. Debaillie**, **J. Craninckx**, **C. Lavin**, **C. Palacios**, **S. Malotaux**, **J. Long**, **D. van den Broek**, and **E. Klumperink**, RF self-interference cancellation

for full-duplex. *In Cognitive Radio Oriented Wireless Networks and Communications (CROWNCOM), 2014 9th International Conference on*. IEEE, 2014.

# LIST OF PAPERS BASED ON THESIS

1. Arjun Nadh, **Joseph Samuel**, Ankit Sharma, S. Aniruddhan, Radha Krishna Ganti, A Linearization Technique for Self-Interference Cancellation in Full-Duplex Radios, submitted to *IEEE Transactions on Wireless Communications*, May 2016. arXiv preprint `http://arxiv.org/abs/1605.01345`